Effect of design and tensile testing specimen geometry on final tensile properties of powder bed fusion plastic

Dean Kouprianoff [1*], and *Karabo* Moore [1]

[1]Department of Mechanical and Mechatronics Engineering, Central University of Technology, South Africa

Abstract

In Laser Powder Bed Fusion there are certain considerations that need to be accounted for when designing for thin-walled or complex shapes. Much is known of how parameters such as build orientation and scanning strategy can affect the resultant tensile properties. The tensile property results are also influenced by factors such as the shape of the specimen. The specimens' cross-sectional geometry and length ratio are carefully considered to obtain accurate and reliable tensile properties. Eighteen different tensile geometries were manufactured using an EOS P110 and PA12 powder. These different geometries were chosen to evaluate different influencing factors such as width, gauge length, specimen geometry and scanning strategy. This knowledge is used in conventional standards when determining specimen geometries. This work aims to combine conventional tensile specimen shape and L-PBF factors to best represent the actual tensile properties of different polymer geometries.

1 Introduction

It is well known that the scanning strategy and build orientation affects the tensile properties during Additive Manufacturing (AM). For Laser Powder Bed Fusion (L-PBF) of polyamide 12 (PA12), the proportion of crystallinity and amorphous regions determines the resulting tensile properties. The amount of crystallinity present is dependent on many factors including aging of the powder and scanning strategy [1]. For polyamide the temperature cycle greatly affects the $\alpha + \gamma$ crystal ratio [2]. In L-PBF, crystallization can take up to several layers to complete depending on the temperature profile in the build [3]. Variations in the reported tensile properties are not only due to L-PBF processes, but also due to the tensile testing's dependency on sample geometry. The elongation measurements during tensile testing are affected by the specimens' gauge length and/or cross-sectional geometry, this is due to local deformation in the necking area and follows Barba's law [4] which states that geometrically similar specimens develop geometrically similar necking regions.

* Corresponding author:

The aim of this work is to describe the relationship between phenomena such as Barba's law and L-PBF building parameters for PA12. These established relationships can further be used during Design for Additive Manufacturing (DfAM).

2 Methodology

Eighteen different tensile geometries were manufactured using an EOS P110 and PA12 powder (PA2200, EOS GmbH). These different geometries were chosen to evaluate different influencing factors such as width, gauge length, specimen geometry and scanning strategy. This information will be useful to know how certain factors pertaining to AM will influence the resulting material properties. For each influencing factor being tested, that factor would be changed while the other variables were kept constant (Table 1). The standard ASTM D638 geometries were used as a base from which to work [5]. ASTM D638 Type 2, 4 and 5 were included for comparison.

Table 1 : Tensile sample geometry dimensions and factors

Sample	Variable	ASTM D638	Width	Thickness	Length	SGR
1	Width	-	**10**	4	25	0,25
2		-	**8**	4	25	0,23
3		Type 4	**6**	4	25	0,20
4		-	**4**	4	25	0,16
5		-	**2**	4	25	0,11
6	Gauge length	-	6	4	**7,62**	0,64
7		-	6	4	**15**	0,33
8		Type 4	6	4	**25**	0,20
9		-	6	4	**35**	0,14
10		Type 2	6	4	**50**	0,10
11	Extreme SGR	-	5	4	10	**0,45**
12		-	4	4	50	**0,08**
13		-	4	16	100	**0,08**
14	Contour/core ratio	-	**0,6**	4	25	0,06
15		-	**0,8**	4	25	0,07
16		-	**1**	4	25	0,08
17		-	**1,2**	4	25	0,09
18	ASTM V	**Type 5**	3,18	4	7,62	0,47

When increasing the gauge length (GL) the narrow section was increased proportionally. For all samples, three tensile specimens were tested at a strain rate of 0.15/min. The specimen geometry ratio (SGR) was calculated by taking the square of the area over the gauge length. For consistency all samples were produced in a single build in the same orientation.

3 Results and Discussion

Figure 1 shows the strong relationship between the specimen geometry ratio and the elongation values (standard deviation in error bars). There is linear relationship between the SGR and the elongation values. The equation in Figure 1 can be used to predict the elongation

for different geometries. The elongation value for ASTM Type 3, which is not included in this work can be predicted. The Type 3 has a width and gauge length of 19 mm and 50 mm respectively; taking the SGR of 0.17 will result in an elongation equal to 18.16% and this agrees well with Lamens et. al. [6] that measured 15.46 ± 3.69% for Type 3. Barbra's law holds very well for the obtained elongation results. At very low SGR the elongation deviates from the trend and was exclude form the trend line data. This will be discussed later.

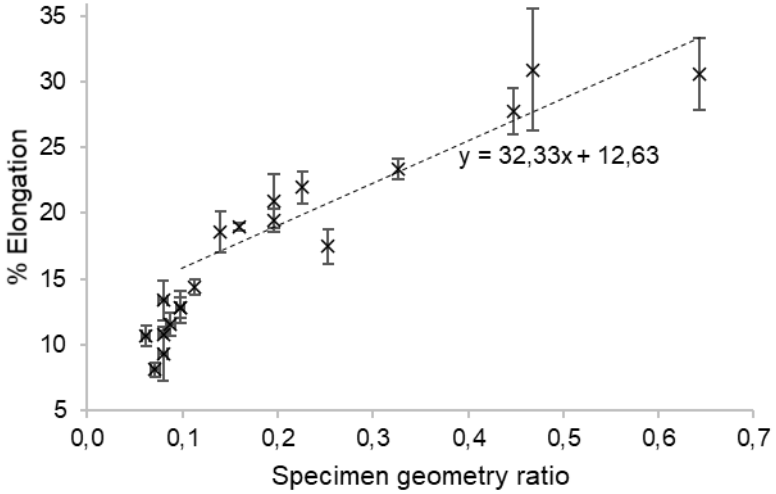

Figure 1: % Elongation vs Specimen Geometry Ratio

As expected, the SGR does not have any definite relationship to the strength of the material (Figure 2). This is because the SGR only considers the localized necking of the tensile specimen.

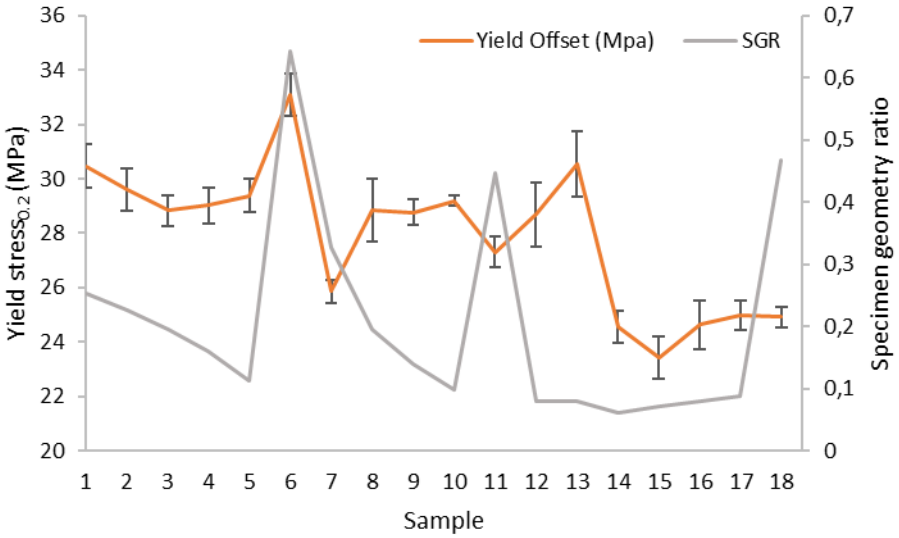

Figure 2: Yield stress and Specimen geometry factor for each sample set

The width however does show a trend with strength of the samples. In Figure 3 the average UTS and Width are plotted against the sample sets.

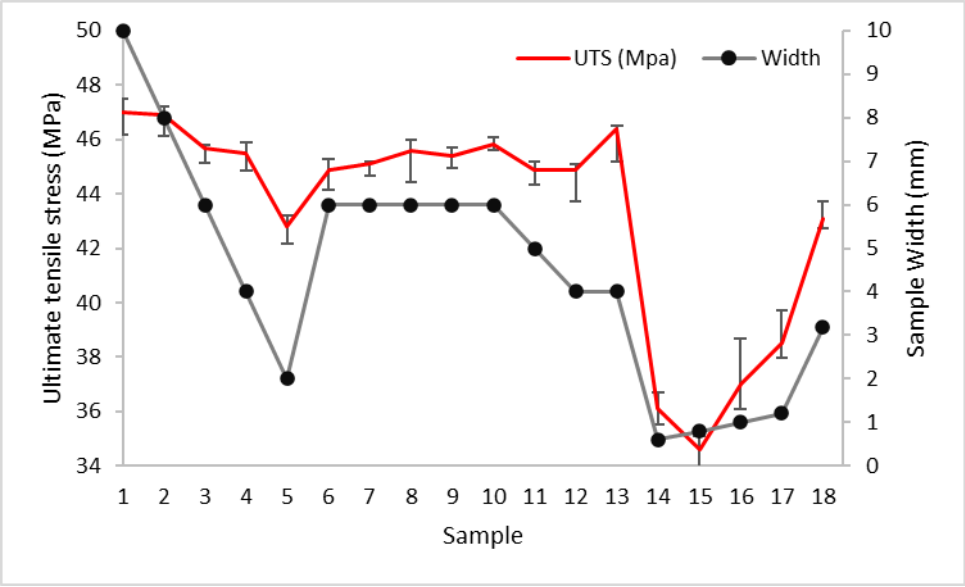

Figure 3: Ultimate tensile stress and specimen width for the different samples sets

In this work the "scanning factor" is calculated by the taking the ratio of the contouring area to the core area. The relatively high drop in UTS seen at sample 14 to 18 in Figure 3 can be attributed to the scanning factor. As the machine uses different scanning strategies such as contouring and core hatching the complex heat history will change the resulting crystalline sizes and in turn the tensile properties [1]. This is largely dependent on the inherent laser parameters such as spot size and beam offset. The default scanning strategy of the EOS P110 can be seen in Figure 4. Note that sample 14 has no core hatching in the narrow section and only consists of contouring while sample 17 starts to show a few hatching lines but still not close to the amount of sample 1.

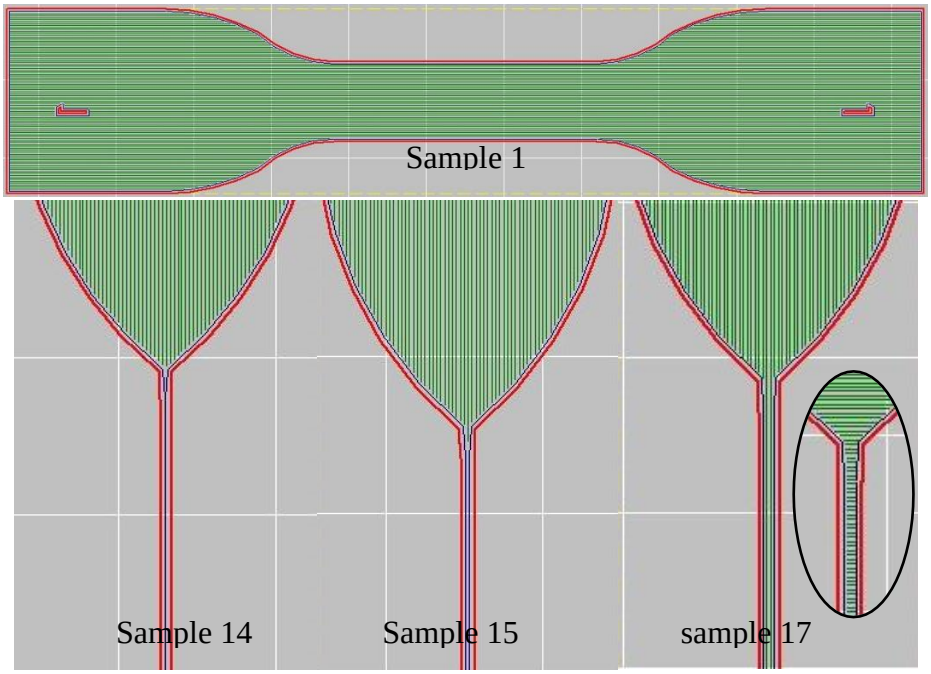

Figure 4: Scanning strategy of a single layer showing Core hatching in the (green) and contouring beam (blue). The next layer of sample 17 showing 90° rotation(balloon bottom right)

With the hatching being 0.25 mm and a laser spot of approximately 0.5 mm it can be expected that a section with a designed width of 0.6 mm will not have core scanning. The scanning strategy of the EOS P110 rotes 90° with each layer meaning that the localized heating will be even higher for layers scanned perpendicular to the narrow section. The rate of crystallization is very sensitive to the temperature and therefore significant effect on the temperature of the narrow samples can be expected [7]. As the wall thickness becomes greater the effect of the contouring becomes less. Another contribution to the scanning factor is the surface roughness/irregularities which for the same reasons plays a more prominent role in the resulting tensile properties of thinner sections [8]. The tensile strength and scanning factor are both plotted against the width and this phenomenon is clearly seen in Figure 5, at low widths the tensile strength reduces but stabilizes beyond 6 mm. This drop in tensile strength can also be attributed to the to the lack of localized necking diminishing strain hardening effects in the thinner sections The samples 0.6 and 10 mm wide has a Scanning factor of 1 and 0.06 respectively.

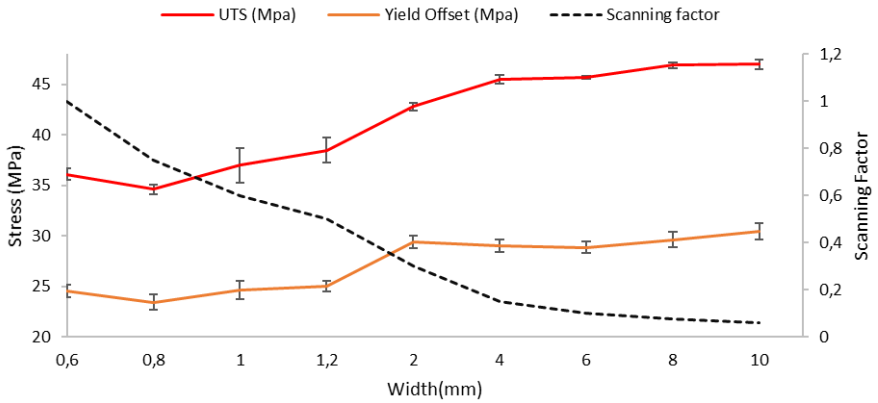

Figure 5: Tensile strength and Scanning factor vs sample width (GL=25 & t=4mm)

For both the yield and ultimate tensile strength, a definite effect on the material properties is observed due to the scanning factor. It is interesting to note that at a scanning factor of around 0.1 and lower, the effect on tensile strength becomes negligible. At higher scanning factors the effect is drastic due to the power-law relationship. This agrees with [9] who found that for thicknesses below 2 mm the tensile properties drastically dropped.

The yield stress is plotted against the elongation for the different samples in Figure 6. As seen previously the sample with the lower SGR has a lower elongation value. The fact that the SGR for sample 14-17 is like that of 10, 12 and 13 (approximately 0.1) it is clear that the strength of the narrower samples is more likely influenced by the scanning factor. Another contributing factor can be the influence of plane stress and strains. The ASTM defines a plastic sample to be thin if the thickness is smaller than 1 mm [10] in which case the ASTM D882 should be used [11]. As expected, the samples with the smallest GL of 7.62 (the ASTM type 5) sample 6 and 18 has the highest measured elongation values but interestingly sample 6 has a considerable higher yield than 18 this can be attributed to both the higher SGR and scanning factor.

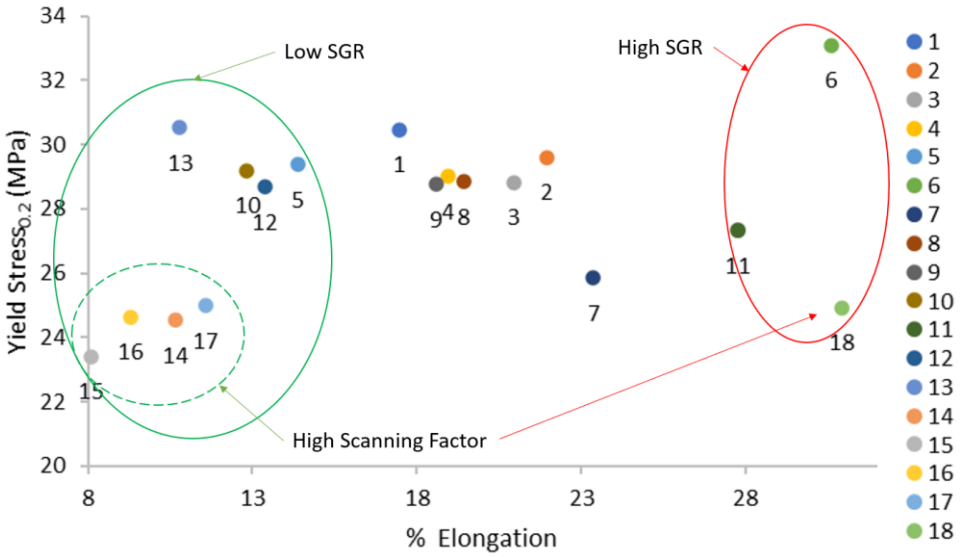

Figure 6: Yield stress vs % elongation of the different samples

In the case that the tensile testing standards are used, it is important to consider that in this single build the ASTM D638 Type 2, 4 and 5 had elongation values of 12.83 ± 1.21, 19.44 ± 2.74 and 30.93 ± 2.20% which is a considerable change in the reported elongation values. For AM smaller specimens are desirable as they lead to reduced printing time and material cost but do have significant higher elongation values. Smaller samples can be used to compare the results from a trendline equation, but great care should be taken if the nature of the fracture and plasticity is not the same. It is desired that the SGR of the specimens be kept the same to be able to accurately compare elongation values.

4 CONCLUSION

The relationship between Barba's law and L-PBF building parameters were described. The linear relationship shown can be used to estimate elongation values for any specimen geometry ratio greater than 0.1. The material properties of L-PBF of polymer PA12 with specific geometries are reported and relationships deduced. The elongation values obtained from the different ASTM D638 sample types vary significantly, ranging from 13 to 30%. The nature of the AM influences the tensile strength when considering the contouring to core ratio. For widths smaller than 2mm the tensile strength can reduce by as much as 10 MPa. These can be used in the design for additive manufactured parts, simulations and interpreting tensile material property data.

5 ACKNOWLEDGEMENTS

This research was supported by the Department of Science and Innovation (DSI) under the Collaborative Program in Additive Manufacturing (CPAM) contract number CSIR-NLC-CPAM-18-MOA-CUT-01. Thanks to the Centre for Rapid Prototyping and Manufacturing (CRPM) and Mr. Wolf Kagisho for his assistance.

6 REFERENCES

[1] S. Dadbakhsh, L. Verbelen, O. Verkinderen, D. Strobbe, P. Van Puyvelde, J. Kruth, European Polymer Journal **92**, 250-262 (2017) https://doi.org/10.1016/j.eurpolymj.2017.05.014

[2] N. Ma, W. Liu, L. Ma, S. He, H. Liu, Z. Zhang, A. Sun, M. Huang, C. Zhu,. e-Polymers **20.1**, 346-352 (2020) https://doi.org/10.1515/epoly-2020-0039

[3] E. Moukhina, N. Rudolph, S. Schmölzer**,** "3D Printing: Crystallization Kinetics of Polyamide 12 during Selective Laser Sintering." *Netzsch (2022)* Accessed: 29 June 2022. https://ta-netzsch.com/3d-printing-crystallization-kinetics-of-polyamide-12-during-selective-laser-sintering

[4] J.R. Davis, Tensile Testing, 2nd Edition, ASM International: Materials Park (2004)

[5] American Society for Testing and Materials. ASTM D638-14. Standard Test Method for Tensile Properties of Plastics. ASTM International, (2014) https://doi.org/10.1520/D0638-14

[6] N. Lammens, M. Kersemans, I. De Baere, W. Van Paepegem, Polymer Testing, **57**, 149-155 (2017) https://doi.org/10.1016/j.polymertesting.2016.11.032

[7] M, Zhao, W. Katrin, D. Dietmar, Polymers **10.2**, 168 (2018) https://doi.org/10.3390/polym10020168

[8] **A. Wörz, D. Drummer,** Understanding hatch-dependent part properties in sls. In proceedings of the Solid Freeform Fabrication Symposium, SFF, 13–15 August 2018, Texas, United states of America (2018) http://dx.doi.org/10.26153/tsw/17150

[9] S. Sindinger, C. Kralovec, D. Tasch, M. Schagerl, Additive Manufacturing, **33**, 101141 (2020), https://doi.org/10.1016/j.addma.2020.101141

[10] American Society for Testing and Materials. ASTM D883-20b. Standard Terminology Relating To Plastics. ASTM International,(2020) https://doi.org/10.1520/D0883-20B

[11] American Society for Testing and Materials. ASTM D882-18. Standard Test Method for Tensile Properties of Thin Plastic Sheeting. ASTM International,(2018). https://doi.org/10.1520/D0882-18